Electronic Supplementary Material (ESI) for Journal of Materials Chemistry C.

Supporting Information

A Wearable, Self-Adhesive, Long-Lastingly Moist and Healable Epidermal Sensor Assembled from Conductive MXene Nanocomposites

Xiaoxuan Wu,[a] Hui Liao,[a] Di Ma,[a] Mingyuan Chao,[a] Yonggang Wang,[a] Xiaolong Jia,*[a] Pengbo Wan*[a] and Liqun Zhang[a]

[a] State Key Laboratory of Organic-Inorganic Composites, Beijing University of Chemical Technology, Beijing 100029, P.R. China. E-mail: jiaxl@mail.buct.edu.cn; pbwan@mail.buct.edu.cn

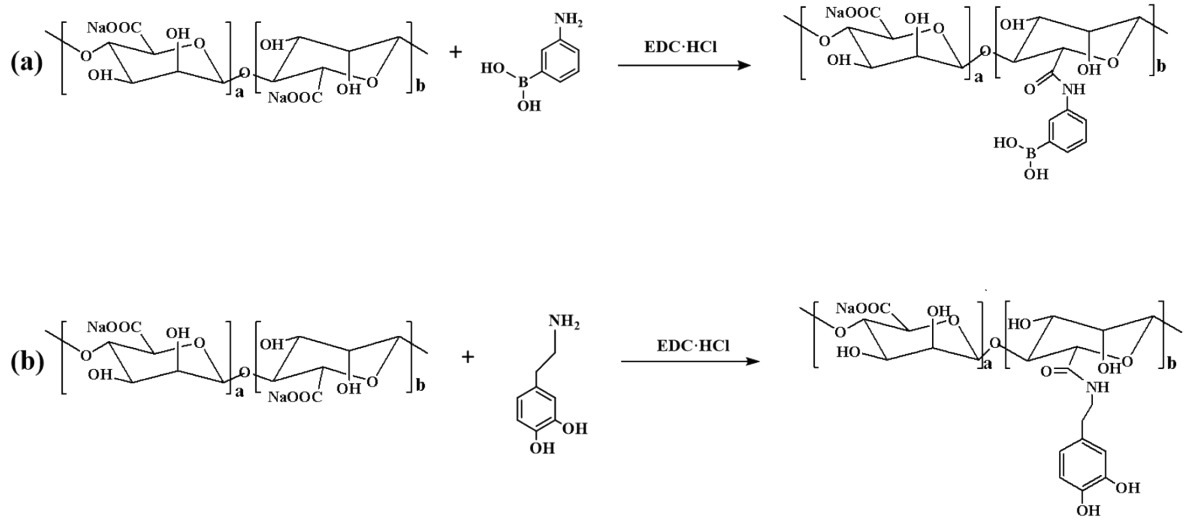

Figure S1. The synthetic routes of (a) Alg-PBA and (b) Alg-DA.

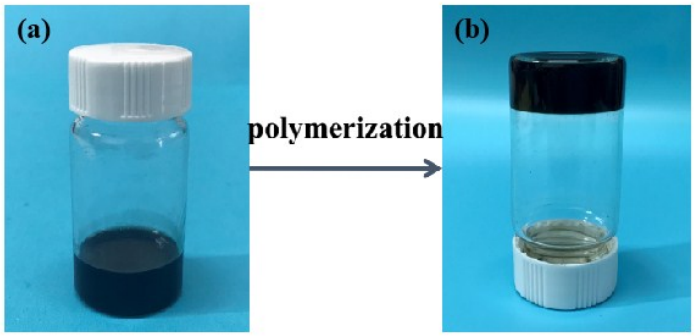

Figure S2. Photographs for the preparation of the MXene nanocomposite organohydrogel. The organohydrogel (a) before and (b) after polymerization.

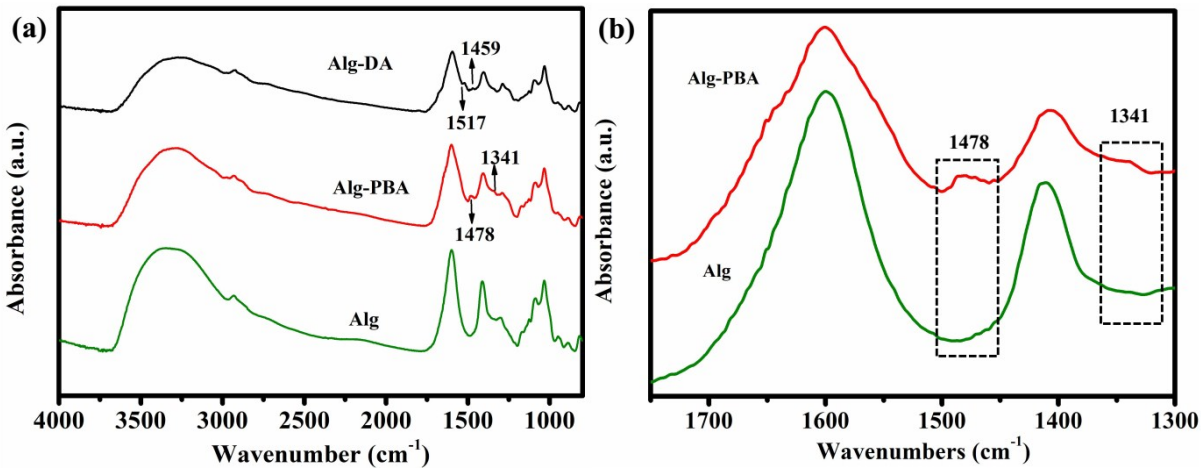

Figure S3. FTIR spectra of Alg-DA, Alg-PBA and Alg.

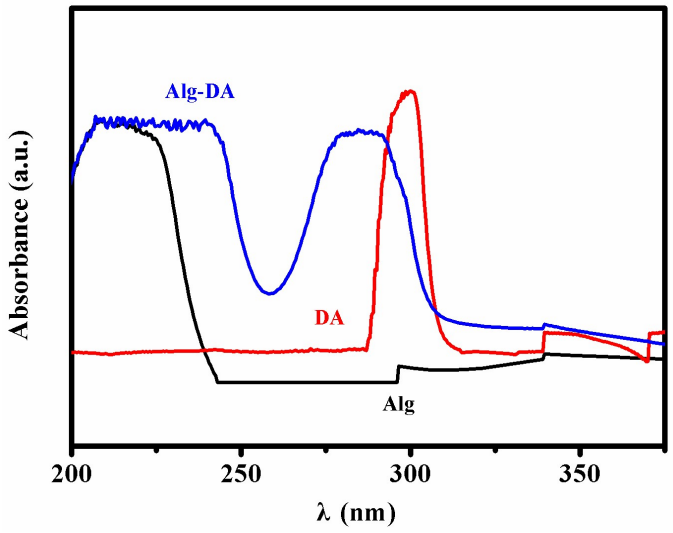

Figure S4. UV-vis spectra of Alg-DA, Alg and DA.

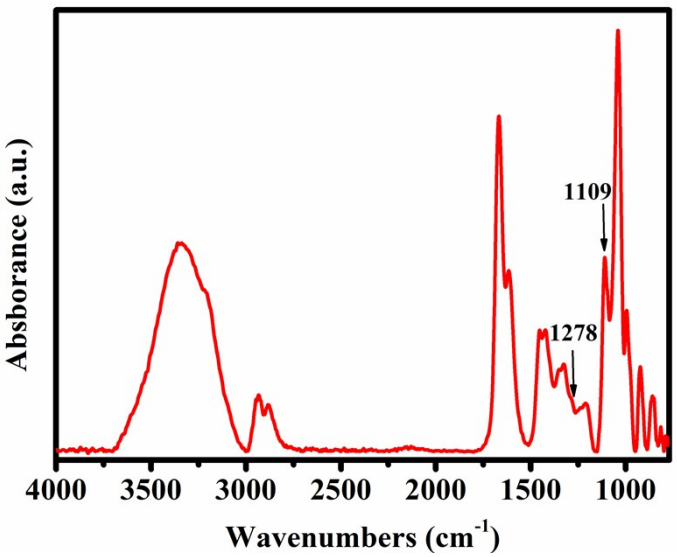

Figure S5. FTIR spectra of MXene nanocomposite organohydrogels.

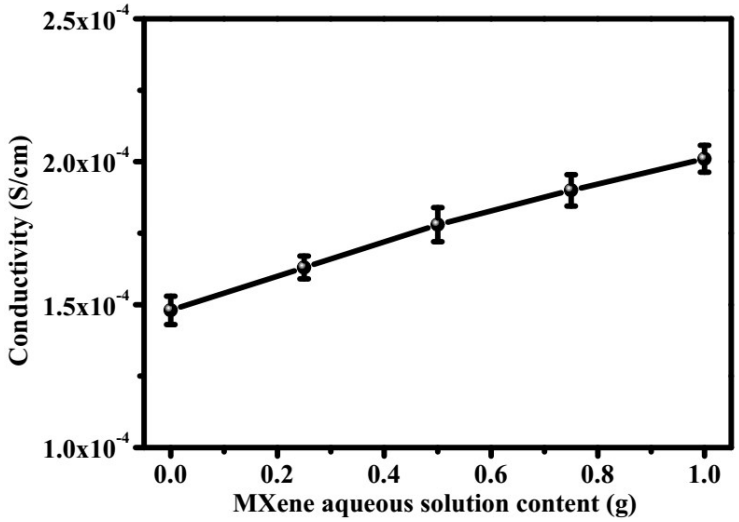

Figure S6. The conductivity of the MXene nanocomposite organohydrogels with different amounts of MXene sheets.

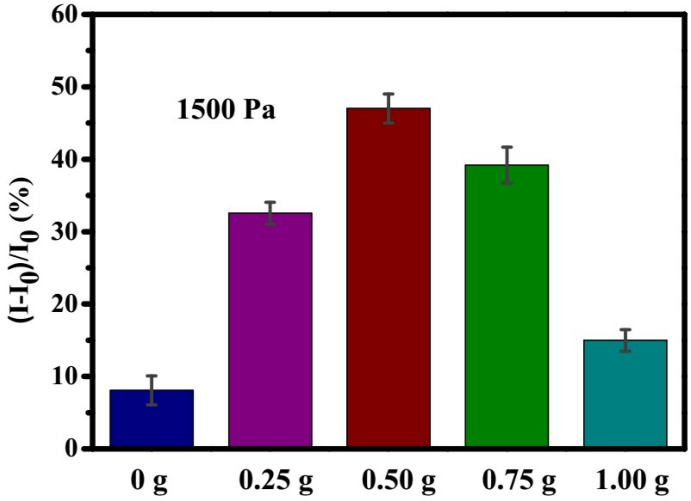

Figure S7. The sensing response of the MXene nanocomposite organohydrogels with different amount of MXene sheets to detect compression deformation (1500 Pa).

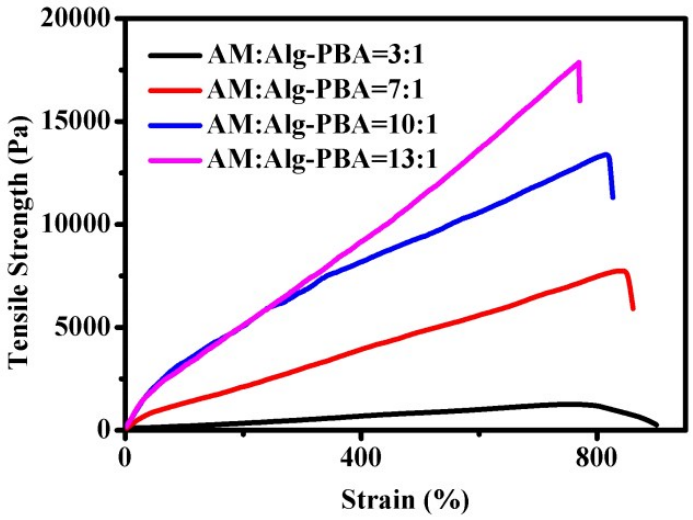

Figure S8. The tensile stress–strain curves of the MXene nanocomposite organohydrogels with different mass ratio of AM to Alg-PBA.

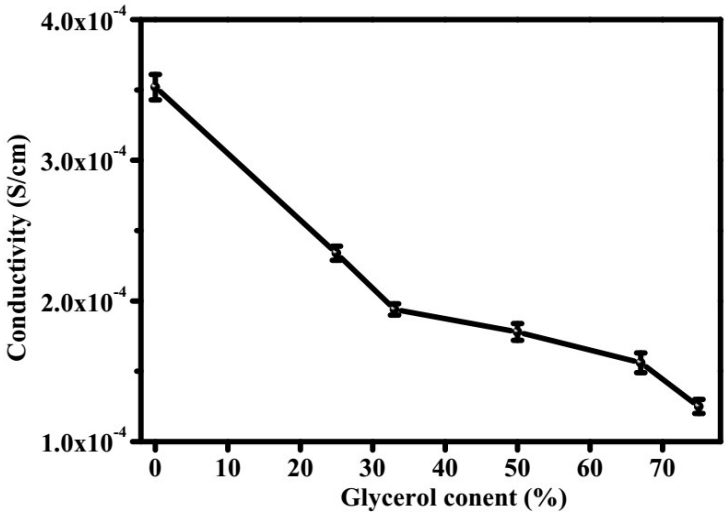

Figure S9. The conductivity of the MXene nanocomposite organohydrogels with different mass ratio of water to glycerol.

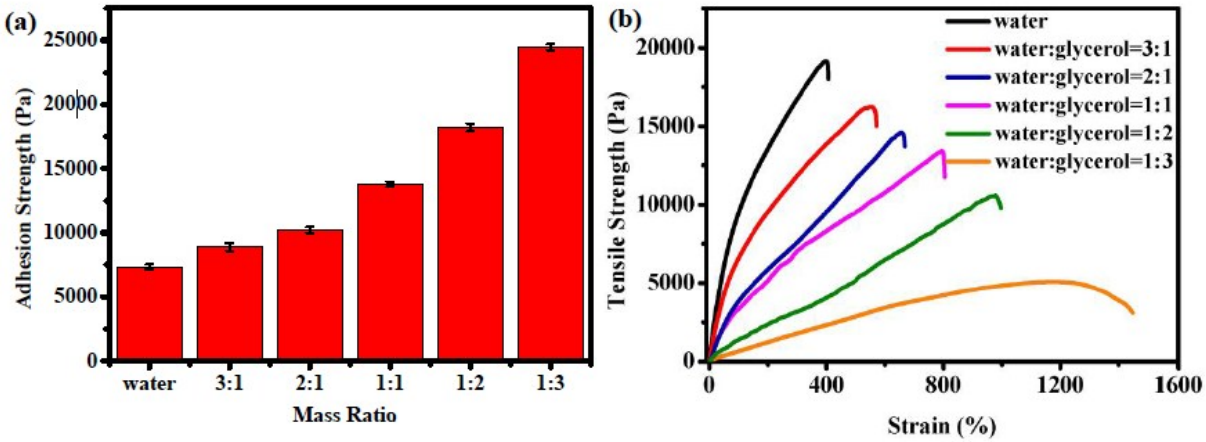

Figure S10. (a) The self-adhesiveness performance and (b) the tensile stress–strain curves of the MXene nanocomposite organohydrogels with different mass ratio of water to glycerol.

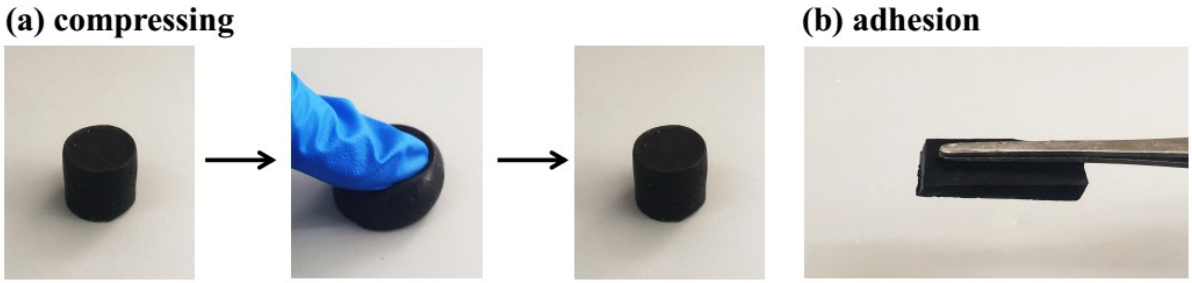

Figure S11. (a) The compression performance and (b) the self-adhesiveness performance of the MXene nanocomposite organohydrogels after stored for 15 days.

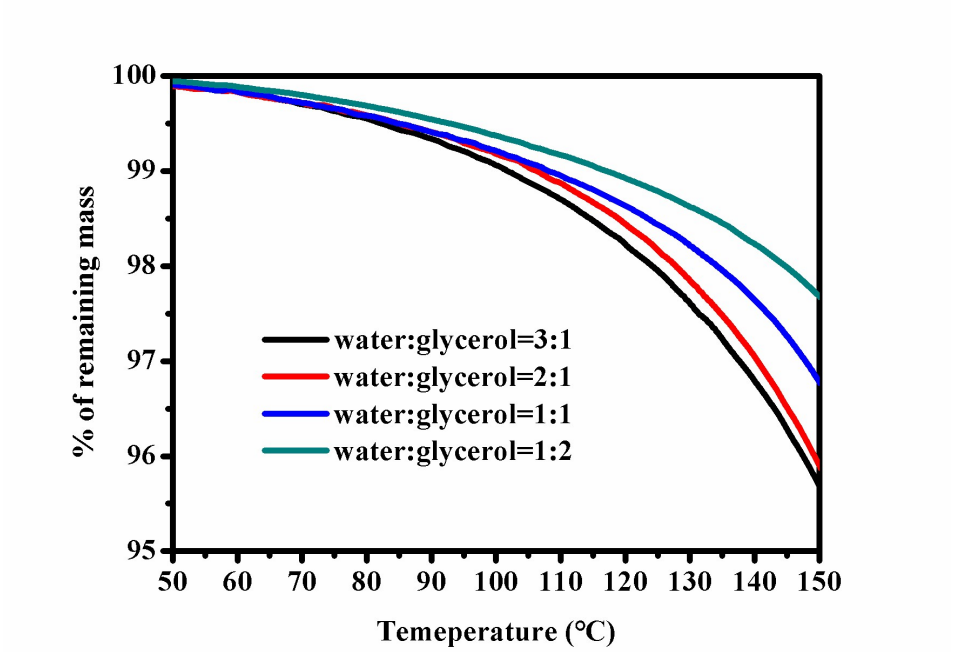

Figure S12. TGA result of the MXene nanocomposite organohydrogels with different contents.

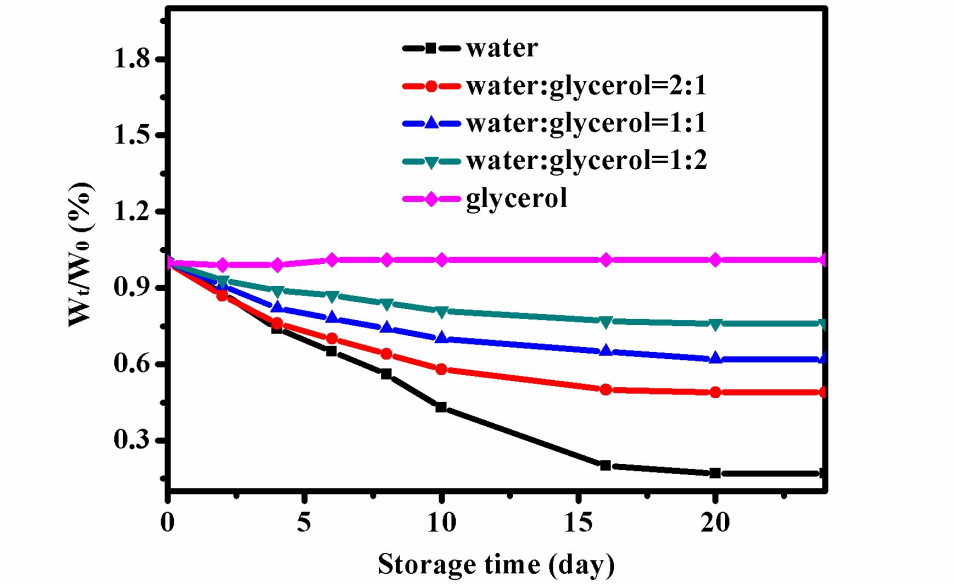

Figure S13. Water loss test of the MXene nanocomposite organohydrogels with different contents at 60 °C for 24 h. W_0 is the original weight of the MXene nanocomposite organohydrogels. W_t is the weight after a certain intervals.

The MXene nanocomposite organohydrogels were placed at 60 °C for 24 h. When the glycerol content increased, the rate of water evaporation decreased (Figure S13). It is ascribed to that the glycerol can form hydrogen bonds with water molecules, which competes hydrogen bonds formed among water molecules and hinders the water evaporation.

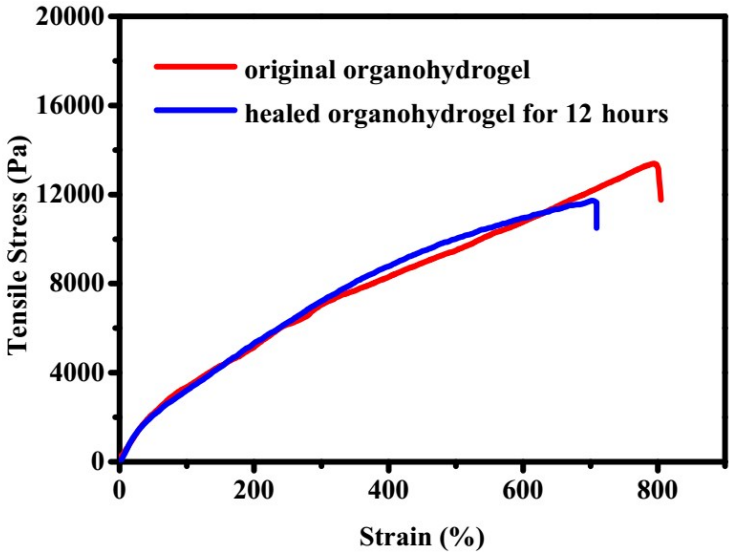

Figure S14. Typical stress-strain curves of the original and the self-healed MXene nanocomposite organohydrogels after self-healing for 12 h.

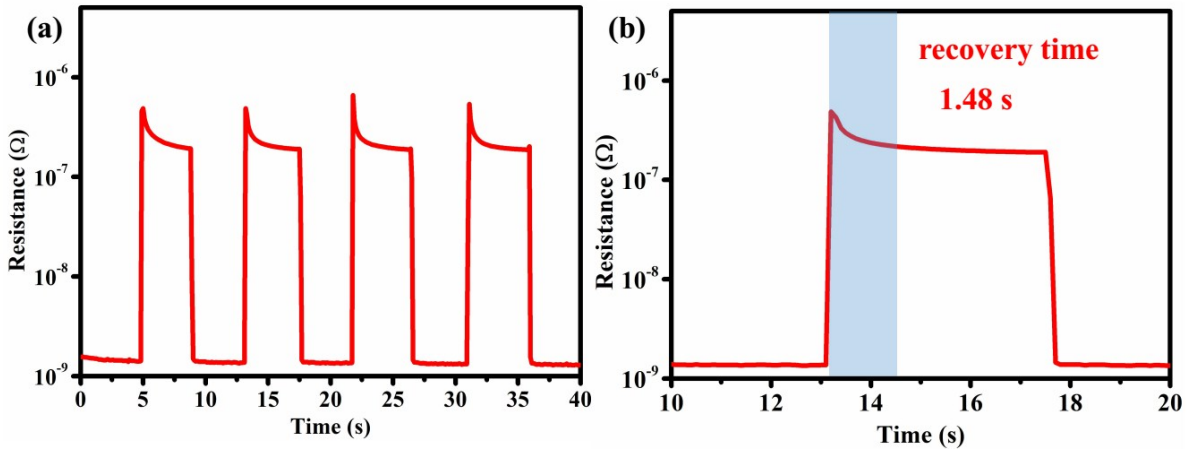

Figure S15. (a) The real-time resistance change when MXene nanocomposite organohydrogels were cut and recombined. (b) The magnified real-time resistance change.

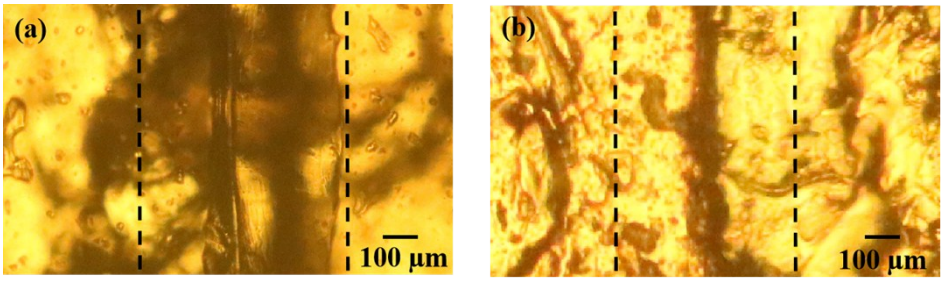

Figure S16. (a) Optical microscopy image of the cut MXene nanocomposite organohydrogel. (b) Optical microscopy image of the self-healed MXene nanocomposite organohydrogels after self-healing for 12 h.

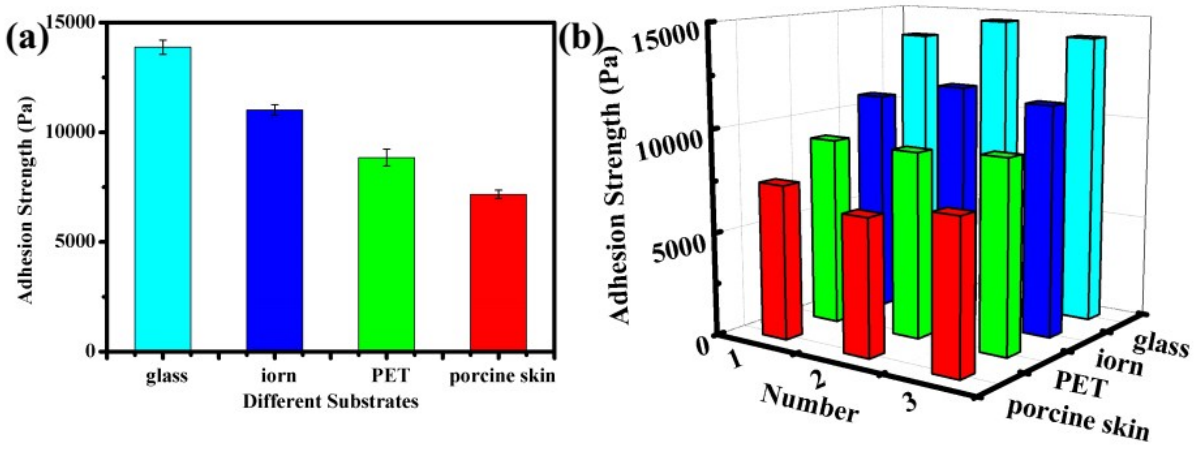

Figure S17. (a) The adhesive strength of the organohydrogels without MXene nanosheets to different substrates. (b) Repeatable adhesion behavior of the adhesive organohydrogels without MXene nanosheets to different substrates (glass, PET, metal and porcine skin).

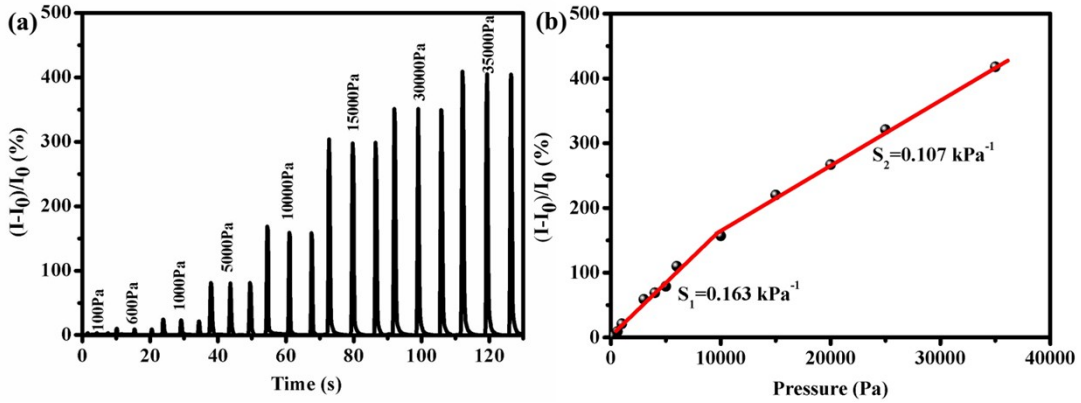

Figure S18. (a) Sensing response of the MXene nanocomposite organohydrogel-based sensors to the different pressures under reversible loading. (b) The sensing sensitivity of the MXene nanocomposite organohydrogel-based sensors.

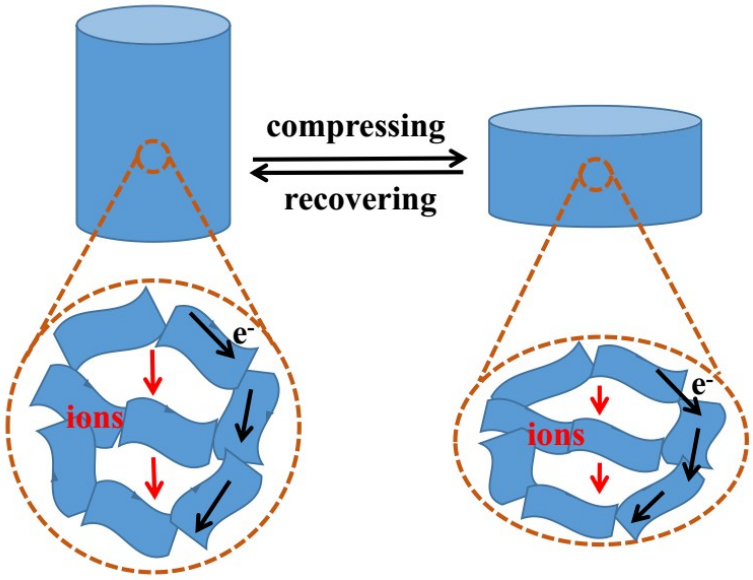

Figure S19. The sensing mechanism of the MXene nanocomposite organohydrogel-based epidermal sensor.

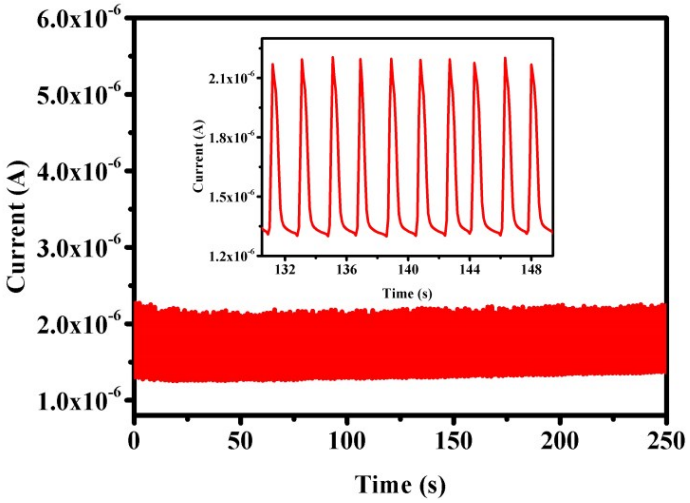

Figure S20. The durability test of the MXene nanocomposite organohydrogel-based sensors. Inset: the detailed durability performance.

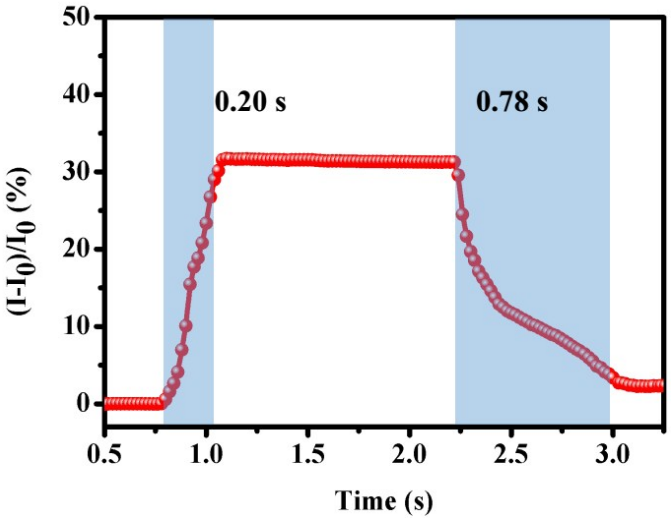

Figure S21. Sensing response time and recovery time for the MXene nanocomposite organohydrogel-based sensors.

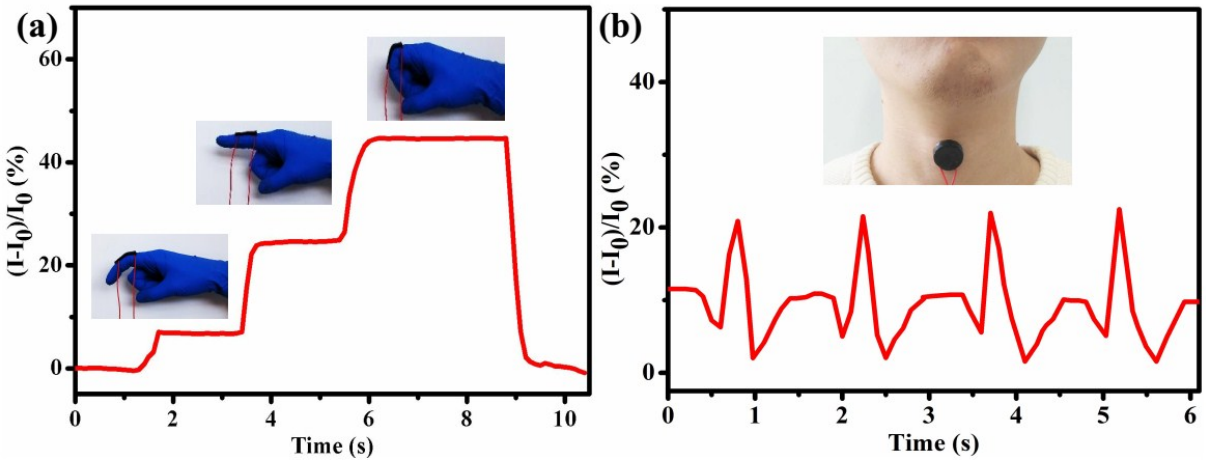

Figure S22. (a) The sensing performance of the sensor adhered to the glove in response to the finger bending at different angles. The insets show the photographs of the sensor attached onto the glove with finger bending at 30°, 60°, and 90°. (b) The sensing performances of the

epidermal sensor in response to the swallowing. The inset shows the picture of the epidermal sensor adhered on the throat.